2011

In-field Jc improvement by oxygen-free pyrene gas diffusion into highly dense MgB2 superconductor

Minoru Maeda
University of Wollongong

Jung Ho Kim
University of Wollongong, jhk@uow.edu.au

Y Zhao
University of Wollongong, yue_zhao@uow.edu.au

Yoon-Uk Heo
Pohang University of Science Technology Pohang, Kyungbuk

K Takase
Nihon University Japan

See next page for additional authors

In-field Jc improvement by oxygen-free pyrene gas diffusion into highly dense MgB2 superconductor

Abstract

Oxygen-free pyrene gas as a carbon (C) dopant was delinked and incorporated into highly dense MgB2 structure via a gas phase diffusion method. The technique offers the advantages that molecular C is homogeneously distributed into MgB2 and substituted at the boron sites without any severe deterioration of grain connectivity. The C substitution causes a significant shrinkage of the a-lattice parameter and an increase in the lattice strain, resulting in high disorder. The introduction of structural disorder as a result of C doping leads to a considerable enhancement of the in-field critical current density (Jc) and upper critical field.

Keywords

field, improvement, oxygen, free, pyrene, gas, diffusion, into, highly, dense, MgB2, superconductor

Disciplines

Engineering | Physical Sciences and Mathematics

Authors

Minoru Maeda, Jung Ho Kim, Y Zhao, Yoon-Uk Heo, K Takase, Y Kubota, C Moriyoshi, F Yoshida, Y Kuroiwa, and S X. Dou

In-field J_c improvement by oxygen-free pyrene gas diffusion into highly dense MgB$_2$ superconductor

M. Maeda,[1] J. H. Kim,[1,a)] Y. Zhao,[1,b)] Y.-U. Heo,[2] K. Takase,[3] Y. Kubota,[3] C. Moriyoshi,[4] F. Yoshida,[4] Y. Kuroiwa,[4] and S. X. Dou[1]

[1]*Institute for Superconducting and Electronic Materials, University of Wollongong, Northfields Avenue, Wollongong, New South Wales 2522, Australia*
[2]*Research Facility Center, Graduate Institute of Ferrous Technology, Pohang University of Science Technology, Pohang, Kyungbuk 790-784, South Korea*
[3]*Department of Physics, College of Science and Technology, Nihon University, 1-8 Kanda-Surugadai, Chiyoda-ku, Tokyo 101-8308, Japan*
[4]*Department of Physical Science, Hiroshima University, 1-3-1 Kagamiyama, Higashi-Hiroshima, Hiroshima 739-8526, Japan*

Oxygen-free pyrene gas as a carbon (C) dopant was delinked and incorporated into highly dense MgB$_2$ structure via a gas phase diffusion method. The technique offers the advantages that molecular C is homogeneously distributed into MgB$_2$ and substituted at the boron sites without any severe deterioration of grain connectivity. The C substitution causes a significant shrinkage of the *a*-lattice parameter and an increase in the lattice strain, resulting in high disorder. The introduction of structural disorder as a result of C doping leads to a considerable enhancement of the in-field critical current density (J_c) and upper critical field. © *2011 American Institute of Physics.* [doi:10.1063/1.3532033]

I. INTRODUCTION

MgB$_2$ is one of the most promising materials for the next generation of superconducting applications because of its high critical transition temperature (T_c) of 39 K (Ref. 1) and lack of weak-links at grain boundaries.[2] However, the in-field critical current density (J_c) still needs to be further improved at its higher operating temperature of $\sim$20 K. In order to achieve this, issues of the grain connectivity and the carbon (C) incorporation into MgB$_2$ material should be addressed. These include (i) grain coupling, (ii) effective cross-sectional area, (iii) impurity phase fraction that disturbs current-flow, and (iv) homogeneous C incorporation into the MgB$_2$ lattice structure.

Homogeneous C incorporation is a critical issue for high magnetic field applications of MgB$_2$. Lattice disorder increases due to C substitution, which causes an enhancement in the upper critical field (B_{c2}) and high-field J_c.[3,4] In contrast, the J_c in self-field decreases because of residual impurity phase and the reduction in effective cross-sectional area. So far, many groups have focused on solid and/or liquid mixing as a processing method for improving the efficiency of C incorporation.[5–9] In particular, the aim of the liquid process is to achieve better mixing among the starting materials.[5] However, agglomeration of unreacted C still exists at the grain boundaries, even after the sintering process. Here, we suggest a method of C substitution via gaseous phase diffusion. The C distribution can be easily achieved by this method and it can be applied widely to bulk, wire, and thin film fabrications for enhancement of J_c.

In our earlier study,[10,11] two-step processing via magne-sium diffusion was suggested to be the easiest way to make a highly dense sample with enhanced low field J_c. In the present work, lumps of pyrene (C$_{16}$H$_{10}$), an oxygen-free hydrocarbon, were selected as a C source in combination to the Mg diffusion process. In this case, atomic or molecular C in gaseous phase diffuses freely and homogeneously in comparison with what occurs in solvent, as reported in carbohydrate doping.[5] By reducing the oxygen content through the use of pyrene which is a highly active C source, it would be more effective in enhancing the J_c. It is thus necessary to evaluate the effects of pyrene gas on the structural parameters, T_c, B_{c2}, J_c, and microstructure of MgB$_2$ systematically.

II. EXPERIMENTAL PROCEDURE

Pyrene lumps (C$_{16}$H$_{10}$, 98%, 1–4 mm) as carbon source were used because of the low boiling temperature of 404 °C and it is a polyaromatic hydrocarbon. In order to explore the possibility of the use of pyrene as C source, two different processes were performed. In the case of study 1, B powder and pyrene lumps were first placed in a Ta tube. It is known that Ta is an absorbing metal for not only oxygen but also hydrogen over a wide temperature range.[12,13] Both ends of the Ta tube were sealed by an arc-welding method in a glove box filled with high purity Ar gas. The sealed Ta tube was then vacuum-sealed in a quartz tube and then sintered at 600 °C for 1 h. This heat-treatment process enables the vaporizing pyrene to treat the surface of the B powder. A compacted slab of the B powder treated in pyrene gas and Mg ingots were put into a Ta tube to undergo the rest of the two-step processing via Mg diffusion. In study 2, the two elements diffused into a compacted B slab simultaneously, i.e., Mg ingots and pyrene lumps were placed in a Ta tube through the same fabrication method used in study 1. A sche-

a)Electronic mail: jhk@uow.edu.au.
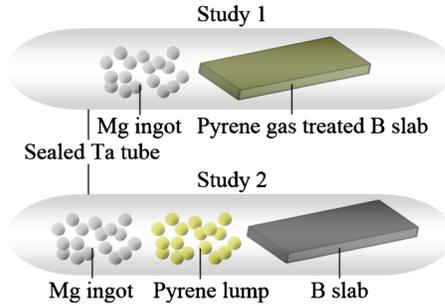b)Electronic mail: yue@uow.edu.au.

FIG. 1. (Color online) Schematic of Mg diffusion method in combination with pyrene gas treatment used in study 1 and study 2. The sealed Ta tubes were vacuum-sealed in quartz tubes, sintered at 1100 °C for 4 min followed by annealing at 660–710 °C for 24–48 h.

matic diagram of the sample preparation is shown in Fig. 1. The proper amount of pyrene in the two studies was chosen to be 2.5 wt % of total MgB_2, because a small quantity of pyrene is sufficient to provide the required amount of C to significantly improve J_c. For reference, an un-doped sample was also prepared from the same Mg diffusion process. Here, Mg ingots (99.99%, 3–5 mm) and amorphous B powder (99.9%, 1 μm) were used as the starting materials. Doped and un-doped samples were sintered for a short period of 4 min at 1100 °C first, followed by the second sintering conditions, namely, 660–710 °C for 24–48 h and 660 °C for 14 h, respectively.

For estimating accurate structural parameters from the Rietveld refinement, high-energy synchrotron radiation (SR) powder diffraction experiments were carried out at the SPring-8 facility in Japan. All samples were also characterized by T_c, J_c, and B_{c2} from magnetic measurements. T_c was determined by ac susceptibility measurements at f =76.97 Hz with $\mu_0 H_{ac}$=50 μT. J_c was calculated from the magnetization hysteresis loops using the Bean critical state model.[14] In addition, B_{c2} was derived from ac susceptibility with f=76.97 Hz, $\mu_0 H_{ac}$=50 μT, and $\mu_0 H_{dc}$=0, 0.2, 0.5, 1, 3, and 5 T. Scanning transmission electron microscopy (STEM) was employed to analyze the morphology, structure, and phase composition.

III. RESULTS AND DISCUSSION

The changes in the lattice parameters with the two different sample preparation methods are presented in Table I. The Rietveld refinement of the crystal structure was carried out with the RIETAN-2000 program.[15] The asymmetric pseudo-Voigt function was used to investigate peak broadening effects caused by crystallite size and microstrain in the crystal lattice.[16] As mentioned in our previous works,[5,9] shrinkage of the *a*-lattice parameter would be strong evidence for C substitution. Interestingly, *a*-lattice parameters for studies 1 and 2 decreased from 3.0834 Å to 3.0713 Å and 3.0756 Å, respectively. It is well known that the actual amount of C can

TABLE I. Results of Rietveld refinement on the high-energy SR powder diffraction data for C-containing gas treated samples and the undoped reference sample. The fitting quality between the observed pattern and the calculated one was evaluated by reliability factors R_{wp}, R_p, and R_I and goodness of fit s.

|	Study 1		Study 2	un-doped
	1100 °C4 min+660 °C48 h	1100 °C4 min+710 °C24 h	1100 °C4 min+710 °C24 h	1100 °C4 min+660 °C14 h
SR powder diffraction experiment				
Radiation source		Synchrotron		
λ (Å)	0.499 19 (5)	0.499 01 (2)	0.499 01 (2)	0.499 19 (5)
$\Delta 2\theta$ (°)		0.01		
Temperature (K)		300		
Reliability factors				
R_{wp}	3.74	3.38	3.23	4.22
R_p	2.77	2.44	2.39	3.12
R_I	3.41	2.30	2.61	4.77
Goodness of fit				
s	1.02	1.16	1.23	0.98
Lattice parameters				
a (Å)	3.069 7 (3)	3.071 3 (4)	3.075 6 (3)	3.083 4 (4)
c (Å)	3.526 2 (2)	3.526 3 (3)	3.529 4 (2)	3.521 4 (3)
Unit cell volume				
V (Å³)	28.776 (4)	28.806 (5)	28.912 (4)	28.994 (5)
Peak broadening coefficients				
X	0.038 0 (3)	0.041 9 (5)	0.036 5 (3)	0.034 6 (5)
Y	0.143 (94)	0.143 (125)	0.143 (57)	0.065 (30)
Mass fractions				
MgB_2 (%)	92.3	93.1	94.7	93.8
MgO (%)	7.7	6.9	5.3	6.2
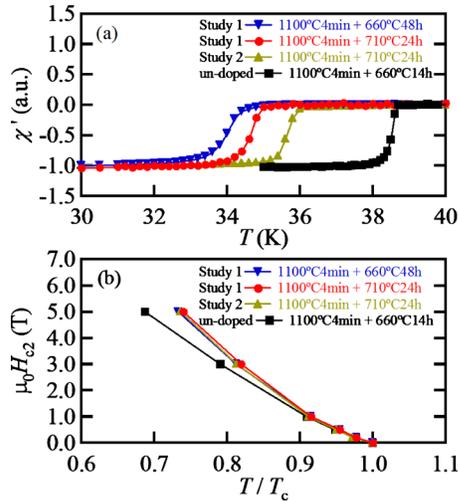
FIG. 2. (Color online) (a) Real component of ac susceptibility with f =76.97 Hz and $\mu_0 H_{ac}$=50 μT at $\mu_0 H_{dc}$=0 T and (b) normalized temperature dependence of B_{c2} derived from ac susceptibility with f=76.97 Hz, $\mu_0 H_{ac}$=50 μT, and $\mu_0 H_{dc}$=0, 0.2, 0.5, 1, 3, and 5 T for C-containing gas treated samples and the un-doped reference sample.

FIG. 3. (Color online) Magnetic field dependence of J_c at 5 and 20 K for C-containing gas treated samples and the un-doped reference sample. The J_c at 4.2 and 20 K for MgB$_2$ thin film is also included for comparison (Ref. 24).

be inferred from the lattice parameters by comparison with the lattice parameters of single crystal.[17] The diffusion process enables C to substitute effectively into the B sites causing significant lattice distortion/disorder. That is to say, the substitution brings lattice strain into the MgB$_2$ due to the difference in atomic radii between C and B. The effective lattice strain is much larger in B layer than that of Mg layer because the effect of C replacing B site will accumulate in the B layer. When the accumulated strain exceeds the critical value, dislocation is formed at the B layer. Contrary to the change in a-lattice, the refined analysis shows a slight increase in c-lattice in pyrene gas treated samples. This may imply that infinitesimal C atoms are inserted at interstitial sites.[18] Direct evidence of structural disorder can be provided by Rietveld refinement of the X and Y profile coefficients,[16,19] which are strongly related to crystallite/ subgrain size and lattice strain, respectively, as shown in Table I. The values of the Y coefficient for studies 1 and 2 are two times higher than for the un-doped sample, even though the ranges of error are relatively high. In contrast, the minor change in the X coefficient means that all samples have nearly the same crystallite size. These facts indicate that the broadening of the MgB$_2$ peak in the SR diffraction patterns for pyrene gas treated samples is mainly caused by strain induced in the crystal lattice. The effect may reduce the unit cell volume, decrease the T_c, and enhance the B_{c2}.

Figure 2 shows the T_c and B_{c2} for all samples. It is noteworthy that the T_c was systematically shifted to lower temperature with decreasing a-lattice parameter [see Fig. 2(a)]. The systematic T_c reduction reflects C substitution and substitutional defects in pyrene gas treated samples, in agreement with the results of Rietveld analysis. Structural disorder effects can be also supported by magnetic B_{c2} curves derived from the ac susceptibility at dc fields from 0 to 5 T and an ac field of 50 μT [see Fig. 2(b)]. The normalized temperature dependence of B_{c2} makes it clear that the slopes for pyrene gas treated samples are steeper in comparison with that of the
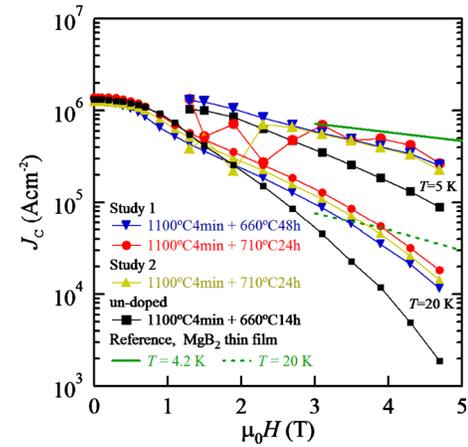
un-doped sample. Interestingly, the curves showed a positive curvature near T_c. The positive curvature of B_{c2} at $T \sim T_c$ indicates that the diffusivity in the σ bands is suppressed compared to that in the π bands.[20] As a result, the enhanced B_{c2} provides an indication of increased two-band impurity scattering, most likely due to the lattice strain induced by C substitution. The structural disorder caused by the localized strain would enhance B_{c2}, resulting in the enhancement of in-field J_c, as shown in Fig. 3.

It is interesting to note that in contrast to the case of any other doping, the self-field J_c at 20 K does not show any difference between the doped and un-doped samples. The main reasons are (i) no significant change in the mass fractions of MgB$_2$ and MgO (Table I) and (ii) the pyrene gas treatment process, i.e., molecular C, does not degrade the connectivity of highly dense MgB$_2$. The active cross sectional area fraction (A$_F$),[21] which is a measure of grain connectivity, can be obtained by

$$A_F = \Delta\rho_{ideal}/(\rho_{300\ K} - \rho_{40\ K}), \qquad (1)$$

where $\rho_{40\ K}$ and $\rho_{300\ K}$ are resistivity values of samples measured at 40 K and 300 K, respectively. $\Delta\rho_{ideal}$ is resistivity difference between 40 and 300 K for a fully connected sample made from a high purity source, such as a dense filament[22,23] made by chemical vapor deposition, for which $\Delta\rho_{ideal}$ is 7.3 $\mu\Omega$ cm. It is well known that a lower value of $\Delta\rho$ indicates good connectivity between grains. Interestingly, A$_F$ of the Mg diffusion sample is comparable to well-connected MgB$_2$ thin film[21] or Mg diffused B whisker.[23] For example, $\Delta\rho$ values of our Mg diffusion samples were estimated to be 9.2–19.0 $\mu\Omega$ cm. Thus, self-field J_c at 20 K reached 10^6 Acm^{-2} and in-field J_c at around 5 T showed 10^4 Acm^{-2}. This result is also comparable to those for MgB$_2$ thin film.[24] To further find other clues, there needs to be deeper insight from the viewpoint of microstructure.

A TEM image of sample for study 1 is shown in Fig. 4(a). This sample which was first sintered at 1100 °C for 4 min followed by second sintering at 710 °C for 24 h showed the best J_c performance. Interestingly, there seems to be no porosity in the matrix. However, such a bright field (BF)-
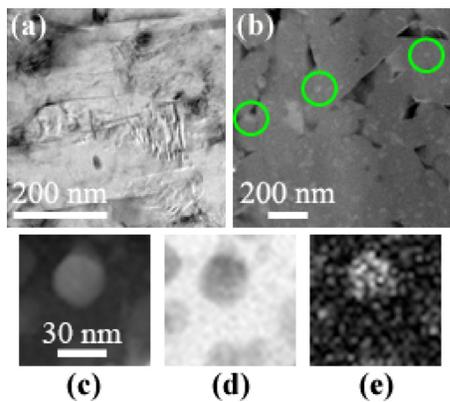
FIG. 4. (Color online) Microstructure of high-density MgB$_2$ bulk prepared from B powder sintered in oxygen-free C-containing gas: (a) BF-TEM image, (b) ADF-STEM image, (c) HAADF-STEM image, (d) B K edge map, and (e) O K edge map.

TEM image does not show impurity phases and grain boundaries. Therefore, an annular dark field (ADF)-STEM and high angle ADF (HAADF)-STEM images of the same sample were captured and they are shown in Figs. 4(b) and 4(c). The ADF-STEM image confirmed that there are many nanoparticles embedded within the MgB$_2$ grains. It is well known that a HAADF-STEM image displays atomic number dependent contrast (Z-contrast) when the sample thickness is uniform.[25] Bright spots correspond to the areas where a high concentration of magnesium (Mg) exists because the atomic number of Mg is higher than those of carbon, boron, and oxygen in this system. In addition, electron energy loss spectroscopy (EELS) maps of B K and O K edges are displayed in Figs. 4(d) and 4(e) to prove the phase identification, respectively. Nanoparticles in a dense MgB$_2$ grain show weak B K and strong O K intensity. Therefore, nanoparticles in the matrix can be related to MgO as shown by green circles [Fig. 4(b)]. The existence of MgO was also confirmed in the high-energy SR powder diffraction results (Table I).

The presence of MgO nanoparticles could enhance the flux pinning effect.[26,27] Since the coherence length in *a-b* plane of MgB$_2$ is about 6–7 nm,[28] a limited amount of inclusions within grains can serve as strong flux pinning centers. The most noticeable feature is that unreacted C agglomeration and impurity phases at grain boundaries are not detected from the EELS maps. This means that our technique of gaseous phase diffusion can efficiently incorporate C into MgB$_2$ structure without any deterioration of grain connectivity.

IV. CONCLUSION

We have demonstrated the influence of C-containing gas on the structural and superconducting properties of highly dense MgB$_2$ bulks synthesized via diffusion process. The C-containing gas penetrated into the MgB$_2$ bulks and caused lattice shrinkage of the *a*-lattice parameter and high disorder in the lattice structure, resulting in significant enhancement of B_{c2} and J_c. Self-field J_c at 20 K reached 10^6 Acm^{-2}, which is quite comparable to the performance of MgB$_2$ thin film. Our gas phase diffusion technique offers a useful pro-

cessing option in various manufacturing processes for MgB$_2$ bulks, wires, and thin films for practical applications.

[1] J. Nagamatsu, N. Nakagawa, T. Muranaka, Y. Zenitani, and J. Akimitsu, Nature (London) **410**, 63 (2001).
[2] D. C. Larbalestier, L. D. Cooley, M. O. Rikel, A. A. Polyanskii, J. Jiang, S. Patnaik, X. Y. Cai, D. M. Feldmann, A. Gurevich, A. A. Squitieri, M. T. Naus, C. B. Eom, E. E. Hellstrom, R. J. Cava, K. A. Regan, N. Rogado, M. A. Hayward, T. He, J. S. Slusky, P. Khalifah, K. Inumaru, and M. Haas, Nature (London) **410**, 186 (2001).
[3] S. M. Kazakov, R. Puzniak, K. Rogacki, A. V. Mironov, N. D. Zhigadlo, J. Jun, C. Soltmann, B. Batlogg, and J. Karpinski, Phys. Rev. B **71**, 024533 (2005).
[4] M. Eisterer, Supercond. Sci. Technol. **20**, R47 (2007).
[5] J. H. Kim, S. Zhou, M. S. A. Hossain, A. V. Pan, and S. X. Dou, Appl. Phys. Lett. **89**, 142505 (2006).
[6] H. Yamada, M. Hirakawa, H. Kumakura, and H. Kitaguchi, Supercond. Sci. Technol. **19**, 175 (2006).
[7] S. X. Dou, S. Soltanian, J. Horvat, X. L. Wang, S. H. Zhou, M. Ionescu, H. K. Liu, P. Munroe, and M. Tomsic, Appl. Phys. Lett. **81**, 3419 (2002).
[8] A. Yamamoto, J. Shimoyama, S. Ueda, I. Iwayama, S. Horii, and K. Kishio, Supercond. Sci. Technol. **18**, 1323 (2005).
[9] J. H. Kim, X. Xu, M. S. A. Hossain, D. Q. Shi, Y. Zhao, X. L. Wang, S. X. Dou, S. Choi, and T. Kiyoshi, Appl. Phys. Lett. **92**, 042506 (2008).
[10] M. Maeda, Y. Zhao, S. X. Dou, Y. Nakayama, T. Kawakami, H. Kobayashi, and Y. Kubota, Supercond. Sci. Technol. **21**, 032004 (2008).
[11] M. Maeda, Y. Zhao, Y. Watanabe, H. Matsuoka, and Y. Kubota, IEEE Trans. Appl. Supercond. **19**, 2763 (2009).
[12] E. Fromm and H. Uchida, J. Less-Common Met. **66**, 77 (1979).
[13] S. Semboshi, N. Masahashi, and S. Hanada, Metall. Mater. Trans. A **34**, 685 (2003).
[14] D. X. Chen and R. B. Goldfarb, J. Appl. Phys. **66**, 2489 (1989).
[15] F. Izumi and T. Ikeda, Mater. Sci. Forum **321–324**, 198 (2000).
[16] P. Thompson, D. E. Cox, and J. B. Hastings, J. Appl. Crystallogr. **20**, 79 (1987).
[17] M. Avdeev, J. D. Jorgensen, R. A. Ribeiro, S. L. Bud'ko, and P. C. Canfield, Physica C **387**, 301 (2003).
[18] A. K. Bengtson, C. W. Bark, J. Giencke, W. Q. Dai, X. X. Xi, C. B. Eom, and D. Morgan, J. Appl. Phys. **107**, 023902 (2010).
[19] A. C. Larson and R. B. Von Dreele, "General structure analysis system (GSAS)," Los Alamos National Laboratory Report No. LAUR 86-748, 2004.
[20] A. Gurevich, Phys. Rev. B **67**, 184515 (2003).
[21] J. M. Rowell, Supercond. Sci. Technol. **16**, R17 (2003).
[22] R. H. T. Wilke, S. L. Bud'ko, P. C. Canfield, D. K. Finnemore, R. J. Suplinskas, and S. T. Hannahs, Physica C **424**, 1 (2005).
[23] P. C. Canfield, D. K. Finnemore, S. L. Bud'ko, J. E. Ostenson, G. Lapertot, C. E. Cunningham, and C. Petrovic, Phys. Rev. Lett. **86**, 2423 (2001).
[24] A. Matsumoto, Y. Kobayashi, K. Takahashi, H. Kumakura, and H. Kitaguchi, Appl. Phys. Express **1**, 021702 (2008).
[25] S. Hata, T. Yoshidome, H. Sosiati, Y. Tomokiyo, N. Kuwano, A. Matsumoto, H. Kitaguchi, and H. Kumakura, Supercond. Sci. Technol. **19**, 161 (2006).
[26] A. Gurevich, S. Patnaik, V. Braccini, K. H. Kim, C. Mielke, X. Song, L. D. Cooley, S. D. Bu, D. M. Kim, J. H. Choi, L. J. Belenky, J. Giencke, M. K. Lee, W. Tian, X. Q. Pan, A. Siri, E. E. Hellstrom, C. B. Eom, and D. C. Larbalestier, Supercond. Sci. Technol. **17**, 278 (2004).
[27] R. K. Singh, Y. Shen, R. Gandikota, C. Carvalho, J. M. Rowell, and N. Newman, Appl. Phys. Lett. **93**, 242504 (2008).
[28] D. Larbalestier, A. Gurevich, D. M. Feldmann, and A. Polyanskii, Nature (London) **414**, 368 (2001).